Early Universe: CMB physics

1 Disclaimer

Discussuion taken from Barbara Ryden [1] and Daniel Baumann [2] books

$$T_0 = 2.7255K, \tag{1}$$
$$\eta_B = 6.1 \times 10^{-10}. \tag{2}$$

2 Equilibrium dynamics

Thompson cross section associated to the elastic scattering $e + \gamma \leftrightarrow e + \gamma$ is

$$\sigma_T = \frac{8\pi}{3}\left(\frac{\alpha_{EM}\hbar c}{m_e c^2}\right)^2 = 6.65 \times 10^{-29}\,\mathrm{m}^2 = 2 \times 10^{-3}\,\mathrm{MeV}^{-2}. \tag{3}$$

. The interaction rate of photons with electrons depends on the electron number density n_e and σ_T as follows

$$\Gamma_\gamma(T) = n_e(T)\,\sigma_T\,c. \tag{4}$$

When the the Universe is fully ionized $n_e = n_p = n_B = n_{B,0}/a^3$, then

$$\Gamma_\gamma(z) = \frac{\Omega_{B,0}\rho_{c,0}}{m_p c^2}\,\sigma_T\,c(1+z)^3 = 5.0 \times 10^{-21}(1+z)^3\,\mathrm{s}^{-1}. \tag{5}$$

The Hubble rate before matter-radiation equality reads

$$H_R(z) = H_0\Omega_{R,0}^{1/2}(1+z)^2 = 2.1 \times 10^{-20}(1+z)^2\,\mathrm{s}^{-1}. \tag{6}$$

while just after

$$H_M(z) = H_0\Omega_{M,0}^{1/2}(1+z)^{3/2} = 1.2 \times 10^{-18}(1+z)^{3/2}\,\mathrm{s}^{-1}, \tag{7}$$

or more general

$$H_{RM}(z) = H_0\left[\Omega_{R,0}(1+z)^4 + \Omega_{M,0}(1+z)^3\right]^{1/2}. \tag{8}$$

It follows that assuming equilibrium number densities the photon decoupling would take place at

$$H_{RM}(z_{\mathrm{dec}}^{\mathrm{eq}}) = \Gamma_\gamma(z_{\mathrm{dec}}^{\mathrm{eq}}), \tag{9}$$
$$z_{\mathrm{dec}}^{\mathrm{eq}} \approx 38.5 \tag{10}$$

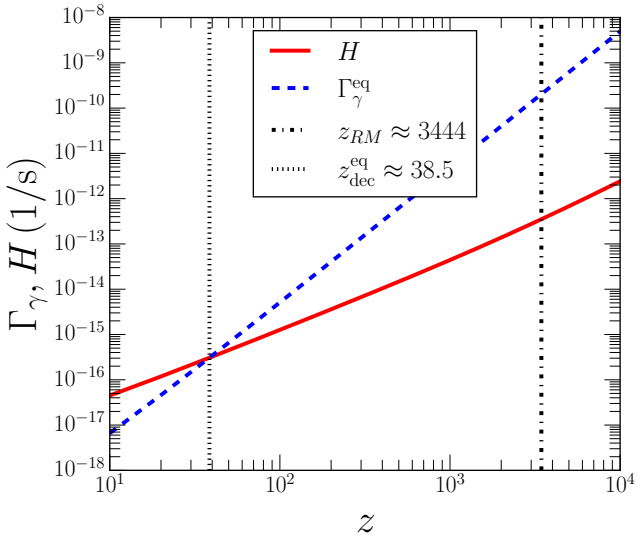

Figure 1: Photon decoupling during equilibrium

3 Recombination

The reactions keeping the formation and destruction of hydrogen atoms on equilibrium are

$$e^- + p^+ \leftrightarrow \mathrm{H} + \gamma. \tag{11}$$

The corresponding equilibrium number densities are

$$n_x^{\rm eq} = g_x \left(\frac{m_x T}{2\pi}\right)^{3/2} e^{(\mu_x - m_x)/T}, \quad x = e, p, \mathrm{H}, \tag{12}$$

$$n_\gamma = \frac{\zeta(3)}{\pi^2} g_\gamma T^3, \tag{13}$$

with $g_\gamma = g_e = g_p = g_{\rm H}/2/2 = 2$. It follows that

$$\left(\frac{n_{\rm H}}{n_e n_p}\right)_{\rm eq} = \frac{g_{\rm H}}{g_e g_p}\left(\frac{m_{\rm H}}{m_p}\right)^{3/2}\left(\frac{2\pi}{T}\right)^{3/2} e^{(m_p + m_e - m_{\rm H})/T} \tag{14}$$

$$\approx \frac{g_{\rm H}}{g_e g_p}\left(\frac{2\pi}{T}\right)^{3/2} e^{E_I/T}, \tag{15}$$

with $E_I = m_p + m_e - m_{\rm H} = 13.6$ eV.

The ionization fraction X_e is defined as

$$X_e = \frac{n_e}{n_p + n_{\rm H}} = \frac{n_p}{n_p + n_{\rm H}} = \frac{n_p}{n_B}, \tag{16}$$

where $n_e = n_p$ and we have assumed $n_p + n_{\rm H} = n_B$. Since $n_B = \eta_B n_\gamma(T)$ we obtain that the expression for X_e at equilibrium, known as Saha equation, reads

$$\frac{1 - X_e^{\rm eq}}{\left(X_e^{\rm eq}\right)^2} = \eta_B \frac{4\sqrt{2}\zeta(3)}{\sqrt{\pi}}\left(\frac{T}{m_e}\right)^{3/2} e^{E_I/T}, \tag{17}$$

whose solution is given by

$$X_e^{\rm eq} = \frac{-1 + \sqrt{1 + 4\alpha(T, \eta_B)}}{2\alpha(T, \eta_B)}, \tag{18}$$

with

$$\alpha(T, \eta_B) = \eta_B \frac{4\sqrt{2}\zeta(3)}{\sqrt{\pi}} \left(\frac{T}{m_e}\right)^{3/2} e^{E_I/T}. \tag{19}$$

The recombination is defined as the moment when $X_e = 0.5$. It follows that the recombination temperature and redshift are

$$T_{\rm rec} = 0.32\,{\rm eV} \simeq 3760\,{\rm K}, \tag{20}$$

$$z_{\rm rec} = \frac{1}{a_{\rm rec}} - 1 = \frac{T_{\rm rec}}{T_0} - 1 \approx 1380. \tag{21}$$

The recombination time can be estimated assuming a matter dominated Universe by that time:

$$t_{\rm rec} = t_0 \left(\frac{a}{a_0}\right)^{3/2} = t_0 (1 + z_{\rm rec})^{-3/2} \approx 270000\,y. \tag{22}$$

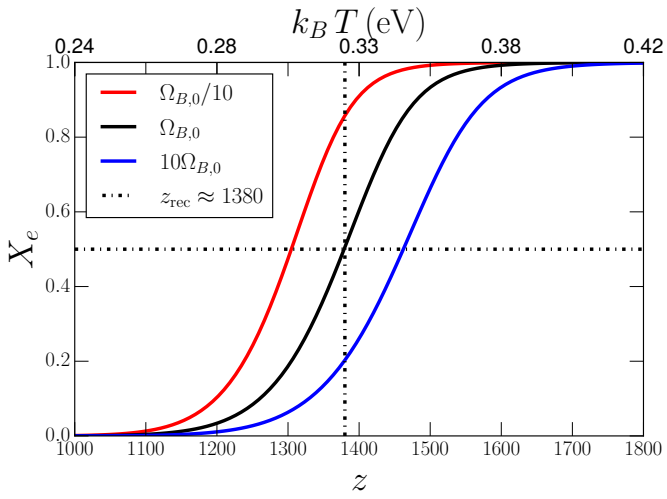

Figure 2: Ionization fraction during recombination

4 Photon decoupling

Taking into account that n_e decreases due to the formation of hydrogen atoms, the photon interaction rate becomes

$$\Gamma_\gamma(z) = n_e \sigma_T \, c = X_e(z) n_B \sigma_T \, c = X_e(z) \frac{\Omega_{B,0}\rho_{c,0}}{m_p c^2} \, \sigma_T \, c(1+z)^3$$
$$= 5.0 \times 10^{-21} X_e(z)(1+z)^3 \, \mathrm{s}^{-1}. \tag{23}$$

The the photon decoupling occurs at

$$H_{RM}(z_{\mathrm{dec}}) = \Gamma_\gamma(z_{\mathrm{dec}}), \tag{24}$$
$$z_{\mathrm{dec}} \approx 1127, \tag{25}$$
$$T_{\mathrm{dec}} \approx 0.265 \, \mathrm{eV}, \tag{26}$$

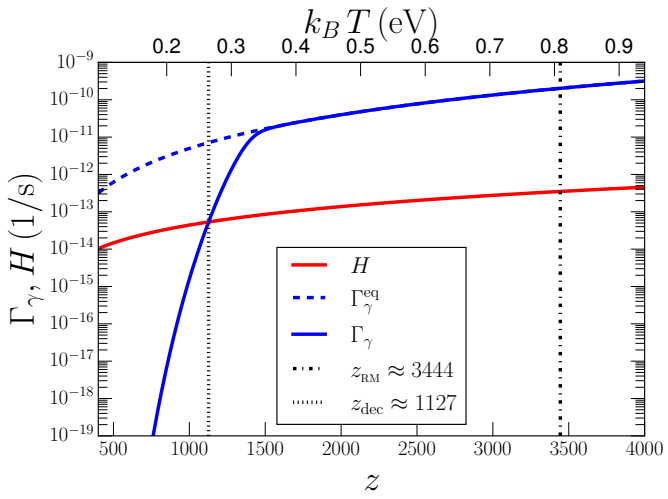

Figure 3: Photon decoupling during recombination

5 Last scattering surface

The expected number of scatterings underwent by a photon from earlier time t until t_0, known as the optical depth, is

$$\tau = \int_t^{t_0} \Gamma_\gamma(t)\, dt = \int_a^1 \frac{\Gamma_\gamma(a)}{a\, H(a)}\, da = \int_0^z \frac{\Gamma_\gamma(z)}{(1+z)\, H(z)}\, dz \tag{27}$$

The time t for which $\tau = 1$ is the time of last scattering, and represents the time that has elapsed since a typical CMB photon last scattered from a free electron. It follows that

$$z_{LSS} \approx 1284. \tag{28}$$

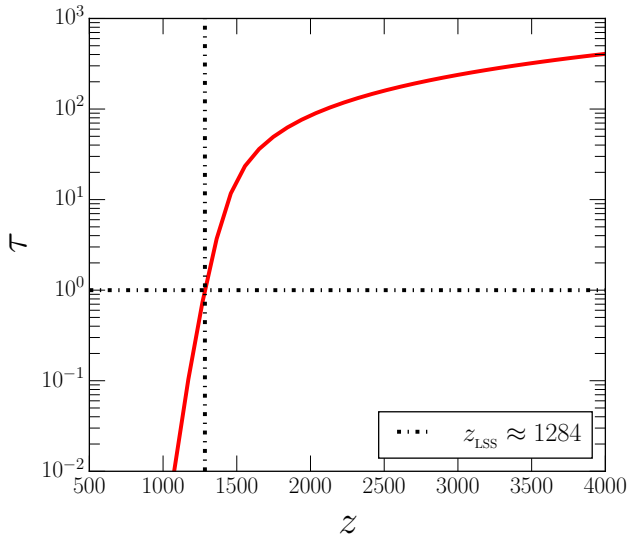

Figure 4: Time of the formation of the last scattering surface

6 Measuring the CMB

The flux of energy across the detector surface (per unit frequency) is

$$I_f = \frac{2h}{c^2} \frac{f^3}{e^{\frac{hf}{k_B T}} - 1}. \tag{29}$$

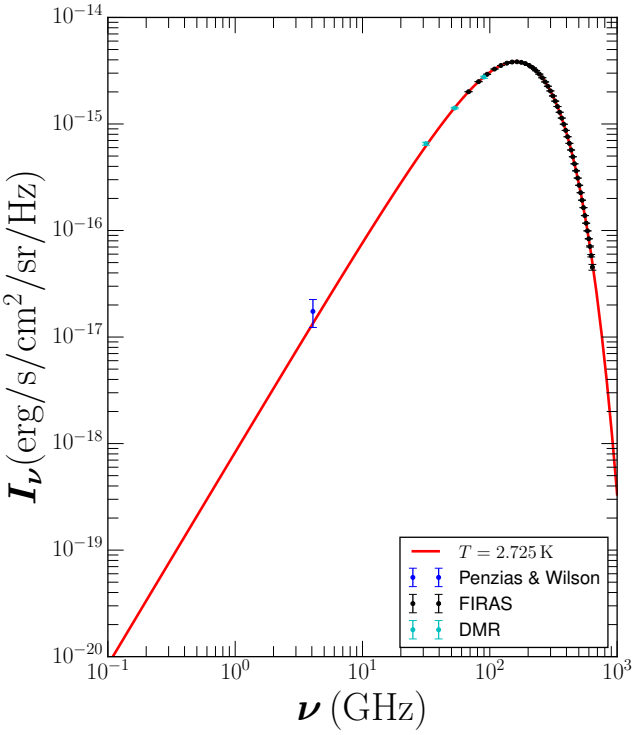

Figure 5: CMB monopole spectrum

7 Size of CMB fluctuations

The angular size $\delta\theta$ of a temperature fluctuation in the CMB is related to a physical size ℓ on the last scattering surface and the angular-diameter distance to the last scattering surface d_A as

$$d_A = \frac{\ell}{\delta\theta} \approx \frac{d_{hor}(t_0)}{z}, \qquad \text{for } z_{lss} \to \infty. \tag{30}$$

Using $d_{hor}(t_0) \approx 14000$ Mpc and $z_{lss} \approx 1090$ it follows that

$$d_A \approx 12.8\,\text{Mpc}. \tag{31}$$

The physical size at the time of last scattering of a fluctuation of angular size $\delta\theta$ becomes

$$\ell(t_{lss}) = d_A\,\delta\theta = 12.8\,\text{Mpc}\left(\frac{\delta\theta}{1\,\text{rad}}\right) = 3.7\,\text{kpc}\left(\frac{\delta\theta}{1\,\text{arcmin}}\right). \tag{32}$$

The resolution of the Planck satellite is

$$\delta\theta_{\text{Planck}} = 5\,\text{arcmin}, \tag{33}$$

which implies a physical size for the fluctuation of the order of

$$\ell(t_{lss}) = 18\,\text{kpc}. \tag{34}$$

This size at present times turns to be

$$\ell(t_0) = \ell(t_{lss})(1 + z_{lss}) \approx 20\,\text{Mpc}. \tag{35}$$

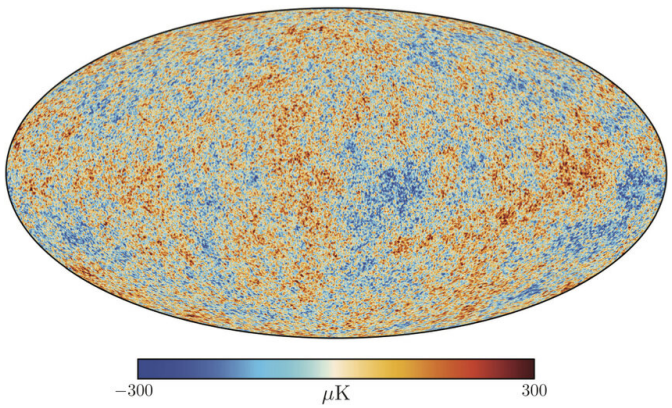

Figure 6: CMB fluctuations

8 Spherical harmonics in the sky

The two-point correlation function

$$\xi(|\vec{x}-\vec{x}'|,t) \equiv \langle \delta(\vec{x},t)\,\delta(\vec{x}',t)\rangle = \int \mathcal{D}\delta\,\mathcal{P}[\delta]\,\delta(\vec{x},t)\,\delta(\vec{x},t)^*, \tag{36}$$

The integral is a functional integral over field configurations and $\mathcal{P}[\delta]$ is the probability of realizing some field configuration $\delta(\vec{x})$. The expectation value $\langle \dots \rangle$ denotes an ensemble average of the stochastic process that created the random field $\delta(\vec{x})$ (e.g. quantum fluctuations during inflation.

The density fluctuations are defined as

$$\frac{\delta T}{T}(\theta,\phi) = \frac{T(\theta,\phi)-T_0}{T(\theta,\phi)} = \sum_{l=0}^{\infty}\sum_{m=-l}^{l} a_{lm}\,Y_{lm}(\theta,\phi). \tag{37}$$

The multipoles l correspond to fluctuations of chararecteristic angular size

$$\delta\theta = \frac{\pi}{l} \tag{38}$$

The correlation function is

$$C(\theta) = \left\langle \frac{\delta T}{T}(\hat{n})\frac{\delta T}{T}(\hat{n}')\right\rangle_{\cos\theta=\hat{n}\cdot\hat{n}'}. \tag{39}$$

The angle brackets denote an average over an ensemble of universes. Of course, our universe is only one member of this ensemble, but we can estimate the ensemble average by dividing the CMB into independent patches and averaging over the correlations in each patch. For large-angle correlations, the number of independent patches is small and this estimate will have a large cosmic variance.

Since the CMB temperature is a real field we have that

$$a_{lm}^* = (-1)^m a_{l,-m} \quad \Rightarrow \quad Y_{lm}^* = (-1)^m Y_{l,-m}. \tag{40}$$

The observational data are consistent with the property that temperature fluctuations $\delta T(\hat{n})$ are Gaussian random field, i.e., that the coefficients $a_{l,m}$ are statistically independent for different l and m,

$$\langle a_{lm} a_{l'm'}^*\rangle = C_{lm}\delta_{ll'}\delta_{mm'}, \tag{41}$$

where brackets mean averaging over an ensemble of Universes like ours. The coefficients C_{lm} do not depend on m in isotropic Universe, $C_{lm} = C_l$. They determine the correlation of temperature fluctuations in different directions:

$$C(\theta) = \sum_{lm}\sum_{l'm'}\langle a_{lm}\,a_{l'm'}^*\rangle\,Y_{lm}(\theta,\phi)\,Y_{l'm'}^*(\theta',\phi') \tag{42}$$

$$= \sum_{l} C_l \sum_{m} Y_{lm}(\theta,\phi)\,Y_{lm}^*(\theta',\phi') \tag{43}$$

$$= \sum_{l=0}^{\infty} C_l \frac{2l+1}{4\pi} P_l(\cos\theta), \tag{44}$$

where $P_l(\cos\theta)$ are Legendre polynomials. Therefore the moments of the angular power spectrum appear as coefficients in an expansion of $C(\theta)$ in terms of Legendre polynomials. Using the orthogonality of the Legendre polynomials, we can also write

$$C_l = 2\pi \int_{-1}^{1} d\cos\theta\, C(\theta)\, P_l(\cos\theta). \tag{45}$$

In this way the information contained in the C_l's is therefore completely equivalent to that of the function $C(\theta)$.

For $\theta = 0$ we obtain that the variance of the temperature anisotropy field is

$$C(0) = \sum_{l=0}^{\infty} C_l \frac{2l+1}{4\pi} P_l(1) = \sum_{l=0}^{\infty} C_l \frac{2l+1}{4\pi} \tag{46}$$

$$= \int \frac{l(l+1)}{2\pi}\, C_l\, d\ln l. \tag{47}$$

Thus, the quantity $\frac{l(l+1)}{2\pi}\, C_l$ determines the contribution to the fluctuation per logarithmic interval of multipoles. The power per logarithmic interval in l is defined as (see Fig. **??**)

$$\Delta_T^2 = \frac{l(l+1)}{2\pi}\, C_l\, T_0^2. \tag{48}$$

The CMB power spectrum will be independent of l if the fluctuations are scale invariant.

9 Acoustic peaks

The horizon distance at the time of the LSS

$$d_{\rm hor}(t_{lss}) = a(t_{lss})\, c \int_0^{t_{\rm lss}} \frac{dt}{a(t)} \tag{49}$$

$$\approx \frac{a(t_{lss})\, c}{2\sqrt{\Omega_{R,0}} H_0} \int_0^{t_{\rm lss}} \frac{dt}{t^{1/2}} = \frac{a(t_{lss})\, c}{2\sqrt{\Omega_{R,0}} H_0}\, 2\, t_{lss}^{1/2} = 2\, c\, t_{lss}. \tag{50}$$

Considering $H^2/H_0^2 = \Omega_{R,0}/a^4 + \Omega_{M,0}/a^3$ gives

$$d_{\rm hor}(t_{lss}) = 2.24\, c\, t_{lss} \approx 0.25\,{\rm Mpc}. \tag{51}$$

A patch of the last scattering surface with this physical size will have an angular size, as seen from Earth, of

$$\theta_{\rm hor} = \frac{d_{\rm hor}(t_{lss})}{d_A} = \frac{0.25\,{\rm Mpc}}{12.8\,{\rm Mpc}} \approx 0.020\,{\rm rad} \approx 1.1^\circ. \tag{52}$$

This angle corresponds to a multipole

$$l_{\rm hor} \sim \frac{180^\circ}{\theta_{\rm hor}} \approx 160. \tag{53}$$

- Sachs-Wolfe region: Large-angle correlations are sourced by fluctuations that were still outside of the horizon at recombination. These fluctuations did not evolve before photon decoupling and are therefore a direct probe of the initial conditions. At t_{lss}

$$\epsilon_{DM} > \epsilon_\gamma > \epsilon_B, \qquad 5.5 : 1.24 : 1. \tag{54}$$

Hence the gravitational potential is dominated by DM. Writing

$$\epsilon_{DM}(\vec{r}) = \bar{\epsilon}_{DM} + \delta\epsilon_{DM}(\vec{r}), \tag{55}$$

it follows that

$$\nabla^2(\delta\Phi) = \frac{4\pi G_N}{c^2}\delta\epsilon_{DM}(\vec{r}). \tag{56}$$

Consider the fate of a CMB photon that happens to be at a local minimum of the potential at the time of last scattering. In climbing out of the potential well, it loses energy, and consequently is redshifted. Conversely, a photon that happens to be at a potential maximum when the universe became transparent gains energy as it falls down the "potential hill," and thus is blueshifted. When we look at the last scattering surface on large angular scales, cool (redshifted) spots correspond to minima in $\delta\Phi$; hot (blueshifted) spots correspond to maxima in $\delta\Phi$. From Sachs and Wolfe calculation,

$$\frac{\delta T}{T} = \frac{1}{3c^2}\delta\Phi. \tag{57}$$

Thus, the temperature fluctuations on large angular scales $\theta > \theta_{\rm hor}$ give us a map of the potential fluctuations $\delta\Phi$ present at the time of last scattering. In particular, the fact that the observed moments Δ_T are constant over a wide range of angular scales, from $l \sim 2$ to $l \sim 40$, tells us that the potential fluctuations were constant over a wide range of physical scales. The creation of temperature fluctuations by variations in the gravitational potential is known generally as the Sachs–Wolfe effect, and the region of the δ_T curve where the temperature fluctuations are nearly constant ($l < 40$) is known as the Sachs–Wolfe plateau.

- Acoustic peaks region: Perturbations with shorter wavelengths entered the horizon before recombination. Inside the horizon the perturbations in the tightly-coupled photon-baryon fluid propagate as sound waves supported by the large photon pressure. The oscillation frequency of these waves is a function of their wavelength, so that different modes are captured at different moments in their evolution when the CMB was released at photon decoupling. This is the origin of the oscillatory pattern seen in the angular power spectrum. The sound horizon distance at the time of last scattering

$$d_s(t_{lss}) = a(t_{lss})\, c \int_0^{t_{\rm lss}} \frac{c_s(t)\, dt}{a(t)} \approx a(t_{lss})\, c \int_0^{t_{\rm lss}} \frac{c/\sqrt{3}\, dt}{a(t)} = \frac{1}{\sqrt{3}} d_{\rm hor}(t_{lss}) = 0.145\,{\rm Mpc}. \tag{58}$$

Hot spots with this physical size have an angular size, as viewed by us today, of

$$\theta_s = \frac{d_s(t_{lss})}{d_A} = \frac{0.145\,{\rm Mpc}}{12.8\,{\rm Mpc}} \approx 0.011\,{\rm rad} \approx 0.7^\circ. \tag{59}$$

- Damping region: On scales smaller than the mean free path of the photons, the random diffusion of the photons can erase the density contrast in the plasma, leading to a damping of the wave amplitudes. This suppresses the amplitude of the CMB power spectrum on small angular scales (large multipole moments).

Event	z	T (eV)	T (K)	t (ky)
Matter-radiation equality	3400	0.81	9390	50
Recombination	1300	0.30	3480	250
Photon decoupling	1100	0.25	2940	380
Last scattering	1100	0.25	2940	380

Table 1: Summary

10 Summary

References

[1] B. Ryden, *Introduction to cosmology*. Cambridge University Press, 1970.

[2] D. Baumann, *Cosmology*. Cambridge University Press, 7, 2022.

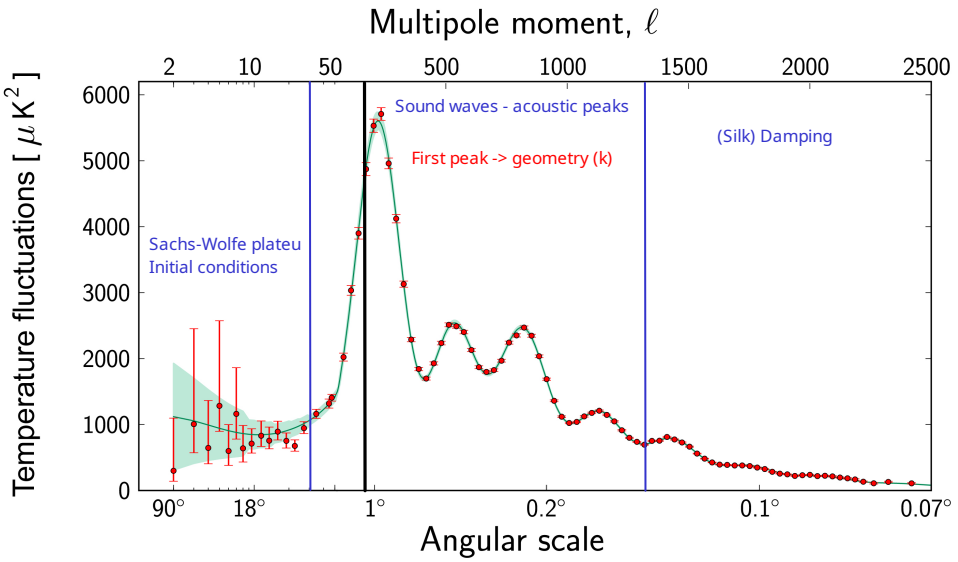

Figure 7: This graph shows the temperature fluctuations in the Cosmic Microwave Background detected by Planck at different angular scales on the sky, starting at ninety degrees on the left side of the graph, through to the smallest scales on the right hand side. The multipole moments corresponding to the various angular scales are indicated at the top of the graph. The red dots are measurements made with Planck; these are shown with error bars that account for measurement errors as well as for an estimate of the uncertainty that is due to the limited number of points in the sky at which it is possible to perform measurements. This so-called cosmic variance is an unavoidable effect that becomes most significant at larger angular scales. The green curve represents the best fit of the 'standard model of cosmology' to the Planck data. The pale green area around the curve shows the predictions of all the variations of the standard model that best agree with the data. While the observations on small and intermediate angular scales agree extremely well with the model predictions, the fluctuations detected on large angular scales on the sky – between 90 and six degrees – are about 10 per cent weaker than the best fit of the standard model to Planck data. At angular scales larger than six degrees, there is one data point that falls well outside the range of allowed models. These anomalies in the Cosmic Microwave Background pattern might challenge the very foundations of cosmology, suggesting that some aspects of the standard model of cosmology may need a rethink.